Sains Malaysiana 48(11)(2019): 2427–2435
http://dx.doi.org/10.17576/jsm-2019-4811-13

Geomagnetic Phenomena Observed by a Temporal Station at Ulu-Slim, Malaysia during the Storm of March 27, 2017

(Fenomena Geomagnetik yang Dicerap oleh Stesen Temporal di Ulu-Slim, Malaysia semasa Ribut pada 27 Mac 2017)

ARAFA-HAMED, T., KHALIL, A.*, NAWAWI, M., HASSAN, H. & M.H. ARIFIN

ABSTRACT

A 3-axis fluxgate magnetometer was temporally setup for continuous recording during March 2017 at 3° 54' 6" N, 101° 29' 41" E, Ulu-Slim, Malaysia. On March 27th, a magnetic storm has been triggered by energetic solar wind emitted from a coronal hole on the sun that impacted the magnetosphere until the end of the measurement campaign on March 29th. The values measured at a sampling rate of 600 Hz are averaged to get a 1 Hz record from March 26 16:00 LT to March 29 12:00 LT. The 1 second data set is studied to deduce all magnetic phenomena captured during the magnetic storm. An overview of the complete record indicates the start of the storm and a complete absence of the typical diurnal variation of the total-field intensity on March 28. The diurnal variations are eliminated by subtracting a moving average of 100 samples from the recorded values. The residual shows a clear amplification of pulsations with the start of the storm. Pulsations enhancement are common around noon and is continuous on March 28th due to magnetotail activities during local night. Magnetospheric breathing as compression and expansion of the magnetosphere at long periods of 20 to 40 min is captured twice during the storm. An obvious occurrence of magnetotail reconnection is deduced by a sudden, steep increase of the total magnetic field with 50 nT at 01:30 LT on March 28. We conclude that the continuous recording of the magnetic field components provides very useful information about what processes are ongoing in space and how it might affect the logistics on the ground. The implementation of similar magnetometers as continuous observation stations would be of crucial benefits for Malaysia in both basic scientific and environmental aspects.

Keywords: Coronal hole; geomagnetic storm; magnetospheric processes

ABSTRAK

Meter Magnet fluxgate 3-paksi telah didirikan untuk rakaman berterusan pada Mac 2017 di 3° 54' 6" U, 101° 29' 41" T, Ulu-Slim, Malaysia. Pada 27 Mac, ribut magnet telah dicetuskan oleh angin suria bertenaga yang dipancarkan daripada lubang korona di matahari yang memberi kesan kepada magnetosfera sehingga berakhirnya kempen pengukuran pada 29 Mac. Nilai-nilai yang diukur pada kadar persampelan 600 Hz adalah untuk mendapatkan rekod purata 1 Hz dari 26 Mac 16:00 waktu tempatan hingga 29 Mac 12:00 waktu tempatan. Set data 1 saat dikaji untuk menyimpulkan semua fenomena magnet yang direkod semasa ribut magnet. Gambaran keseluruhan rekod lengkap menandakan permulaan ribut dan ketiadaan lengkap variasi diurnal yang tipikal daripada keamatan keseluruhan medan pada 28 Mac. Variasi diurnal dihapuskan dengan menolak purata bergerak 100 sampel daripada nilai yang direkodkan. Baki menunjukkan penguatan denyutan yang jelas dengan permulaan ribut. Peningkatan pulsasi adalah umum sekitar tengah hari dan berterusan pada 28 Mac disebabkan aktiviti ekor magnet semasa malam tempatan. Pernafasan magnetosfera sebagai mampatan dan pengembangan magnetosfera pada masa yang panjang iaitu 20 hingga 40 min direkodkan dua kali semasa ribut. Satu kejadian yang jelas mengenai penyambungan semula ekor magnet disimpulkan oleh peningkatan mendadak daripada medan magnet keseluruhan dengan 50 nT pada 01:30 waktu tempatan pada 28 Mac. Kami menyimpulkan bahawa rakaman berterusan komponen magnetik menyediakan maklumat yang sangat berguna tentang apa proses yang berterusan dalam ruang dan bagaimana ia boleh mempengaruhi logistik di lapangan. Pengukuran meter magnet yang sama sebagai stesen pemerhati yang berterusan akan menjadi manfaat penting bagi Malaysia dalam kedua-dua aspek asas saintifik dan alam sekitar.

Kata kunci: Lubang korona; proses magnetosfera; ribut geomagnet

INTRODUCTION

Magnetospheric substorms are known to be caused by the electric fields generated in the magnetosphere by the solar wind interactions. The dynamic collision-less buffeting of the solar wind and the possible injection of charged plasma particles into the magnetosphere are severe storm triggers. During a storm, the magnetosphere suffers induced activities that turn it from a quite one to what is widely called to be a disturbed magnetosphere. Magnetic disturbances are highly variable, some changing on the

scale of seconds, others on the scale of days, and typical disturbance amplitudes on the ground range between a few and some hundred Nanoteslas.

The complex magnetic field lines around the sun play a role in attenuating the charged plasma particles that are usually accelerated by eruptions in the solar magnetosphere. On March 25th the Solar Dynamic Observatory (SDO), run by NASA, observed a region on the sun with no magnetic field lines (Figure 1). Such magnetic openings in the lower solar atmosphere (Figure 1, right) are referred to as 'Coronal holes' and are characterized by fast-moving charged particles (solar-wind) streaming outside the sun.

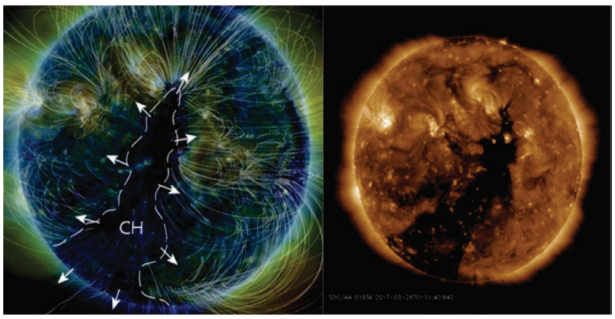

FIGURE 1. Left: the observed absence of magnetic field lines that indicated the existence of a canyon shaped coronal-hole facing the earth on March 25th. Right: image of the wide coronal-hole, which allowed powerful solar wind to flow towards our planet (photographed by NASA's SDO)

As the coronal hole faced the earth, the streaming energetic solar-wind particles hit the planet on March 27th, 2017 and triggered a G2-class geomagnetic storm. Several space weather stations recorded the Earth's response to the event. Figure 3 illustrates an example from northern Norway. Magnetometers indicated a shaking of Earth's magnetic field in response to buffeting from the incoming solar wind stream, while ground-current instruments at the Polar-light-center in Lofoten registered simultaneous enhanced induced currents. Further on March 28th the solar-wind speed has been accelerated to more than 700 km and energized the storm that lasted until the end of March 2017.

A 3-axis fluxgate magnetometer was set up for temporal recording in the frame of a survey campaign at Ulu-Slim in the governorate of Perak, Malaysia and observed the magnetospheric response to the storm of March 27th. The magnetometer was located at a latitude of 3° 54' 6" N, and longitude of 101° 29' 41" E (Figure 2). All of the north component (x), east component (y) and the vertical component (z) are recorded at a sampling frequency of 600 Hz and then averaged to result in a 10 Hz saved data. The magnetometer has a resolution of 1pT and an accuracy of about 10pT @10Hz.

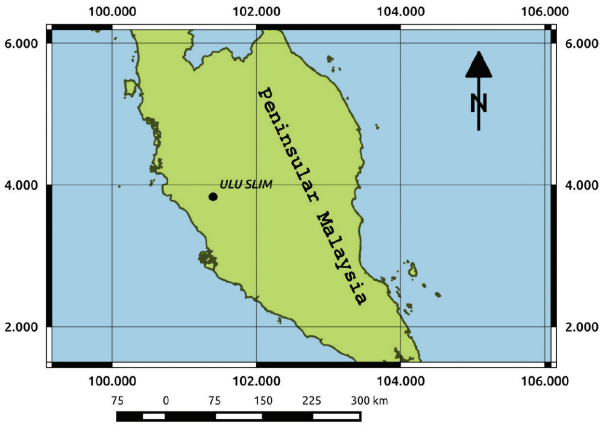

FIGURE 2. Location of the observation site at Kampong Ulu Slim, Perak, Malaysia

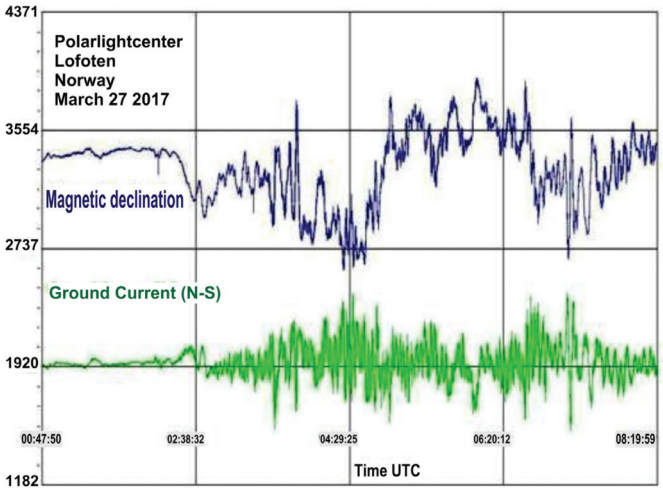

FIGURE 3. Observed activities around the North Pole due to solar-wind interaction on March 27, 2017. Shaking of Earth's magnetic field is observed at northern Norway observatories in response to buffeting from the incoming solar wind stream (blue curve). Ground-Current instruments at the Polar-light-center in Lofoten recorded enhanced induced electric field corresponding to the storm disturbances

OVERVIEW OF THE RECORDED TIME SERIES AND METHODS

The recorded time series starts at 16:00 (LT) on March 26th and continues until 12:00 on March 30th. It comprises three orthogonal magnetic components; north-south (x), east-west (y) and the vertical component (z) (Figure 4). The (x) component has an average value of 41075 nT, the average (y) component is 115 nT, while the mean (z) component is -5740 nT. All average values match with the calculated components of the international geomagnetic reference field (IGRF) at the location of the temporal station in Ulu-Slim references. The observed mean values indicate that most of the magnitude of the total field (**F**) is contained in the horizontal (x) direction. This condition shows characteristic for near equator zones, where the vertical component is minimum and the horizontal component is maximum.

From the start of the considered record up to 08:40 on March 27, all magnetic components were quite with smooth changes that are typical for diurnal variations on magnetosphere quite-days at the station latitude. Both of the x and z components started to increase gradually from 06:00 (LT) in the frame of diurnal variation and the y component started to decrease in the same frame as well. At about 08:40 all components suffered clear intensive disturbances due to the arrival of the solar wind stream at the magnetosphere.

All components indicate that the storm continued until the end of the available records. On March 28th both y and z components show maximum disturbance with the typical diurnal variation can still be observed as long-period changes, while the x component has been completely dominated by the fluctuations of the storm with a total absence of the typical diurnal variation (Figures 4 & 5). This notice concludes that the 28th of March was the core of the magnetic storm after injection of the solar-wind particles into the magnetosphere. On the next 2 days (29th and 30th March) the typical diurnal variations appeared in all components but with superimposed enhanced pulsations that continued until the end of the records.

OBSERVED PHENOMENA

THE ENHANCED OCCURRENCE OF PULSATIONS

Studies about the physics of micropulsations, magnetic pulsations, and ULF waves in the magnetosphere are the earliest subjects of geophysics. The magnetic pulsations have been classified according to their general forms in continuous (Pc) and irregular (Pi) types. Further sub-classifications are then recognized according to the periods of the pulsations and resulted in (Pc1 to Pc5) and (Pi1, Pi2). For more details about magnetic pulsations and its types one can refer to Glassmeier et al. (2009) and McPherron (2005). Modern observatories and satellite measurements showed a more sophisticated grouping and of magnetohydrodynamic (MHD) waves, that reach

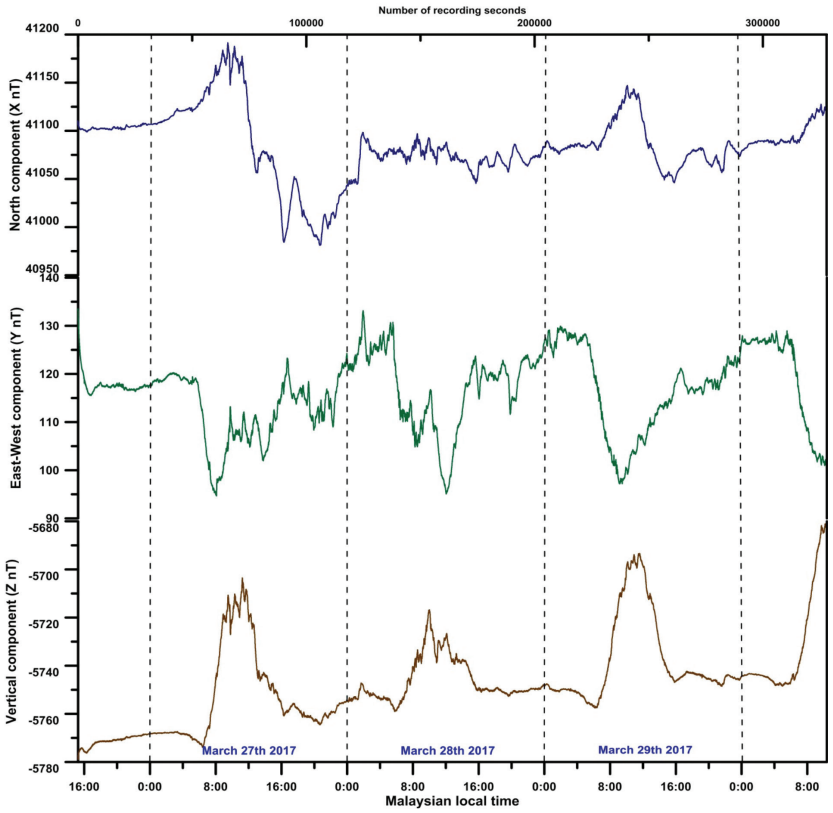

FIGURE 4. The 3 orthogonal magnetic field components recorded during the magnetic storm of March 27th. The curves include the records from local time 16:00 on March 26th to 12:00 on March 30th, the arrival of the solar wind at the magnetosphere started on March 27th at about 08:30 LT

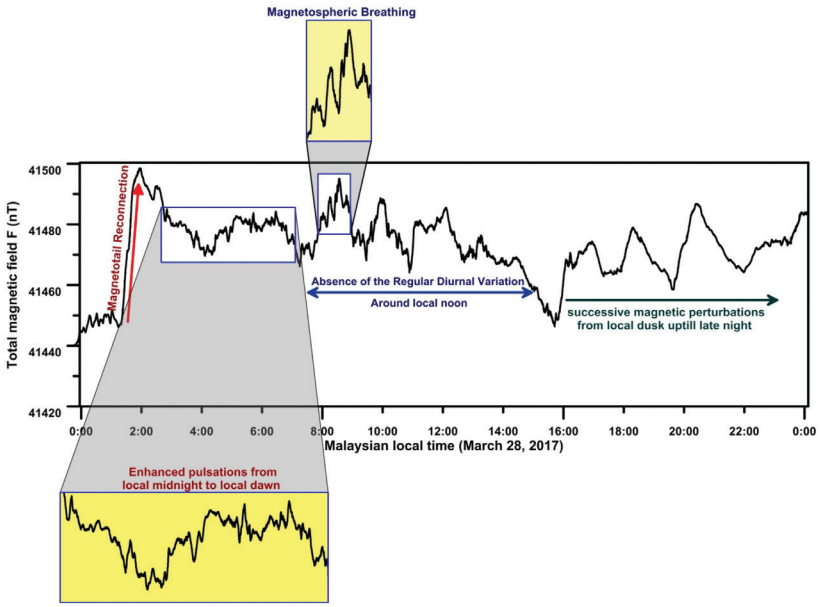

FIGURE 5. Total magnetic field intensity observed on March 28th. The magnetometer captured particular phenomena along its rotation trip from the night-side magnetotail to the dawn then the noon, until the dusk to the night-side again. Magnetotail reconnection, enhanced pulsations, magnetospheric breathing, absence of the typical diurnal variation-cycle and successive perturbation periods can be distinguished on the time series

the Earth's ground. These waves are excited by processes at different distances in the magnetosphere from the solar wind to the ionosphere down to the Earth's surface (Alfven & Falthammar 1963; Baker et al. 1996; Barnes 1983; Nabert et al. 2013). Knowledge of the wave properties and the current state of the sun can give us a clue to what is likely to be occurring at any particular latitude and local time (Ghamry et al. 2016; Lin et al. 1991; Nabert et al. 2017).

The study of magnetic pulsations associated with a geomagnetic storm is typically an important consideration. Pulsations provide additional storm parameters which can be used for more detailed storm classifications. This can in turn showed storm-intervals with special characteristics in respect of pulsations in order to study their relationship with other electromagnetic processes. Moreover, the study of the pulsations-periods and their course of changing observed during a storm leads to a more understanding of MHD theories. In this work, we study the relationship between the pulsations generated during the storm and its indications about the space weather processes over the 3 days of recordings.

Although geomagnetic pulsations are classified as ULF MHD waves, it remains of higher frequency than the very long-period diurnal variations observed at an observatory. Therefore, filtering must be conducted over the entire recorded time series of magnetic data in order to isolate variations with periods within the range of magnetic pulsations. As the data used has a sampling rate of 1Hz then the Pc1 types cannot be considered because of the limited Nyquist frequency.

The high pass filtered data ($\mathbf{F}_{tp}$) has been achieved by constructing a moving average time series with a window of 100 samples which is then subtracted from the measured time series ($\mathbf{F}_t$) (1).

$$F(tp) = Ft - \frac{\sum_{t-50}^{t+50} Ft}{100} \quad (1)$$

The resultant high-frequency signals ($\mathbf{F}_{tp}$) are shown in the upper panel of Figure 6. The first observation from this graph is an obvious amplification of pulsations observed at the storm-onset on March 27 08:40 LT that continued till the end of the record. This is a clear indication about storm-generated pulsations in the magnetosphere. The maximum pulse amplitude is of about 30nT at about 12:00 LT on March 27 that coincide with the existence of the station directly under the subsolar point of the magnetosphere.

The middle panel of Figure 6 displays the power spectrogram (dynamic spectrum) calculated for the pulsation signal using windows of 1024 samples. The spectrogram is useful in reflecting the change in the frequency content of the signal with time (Langangen et al. 2007; Schillinger & Papadopoulos 2010; Schillinger et al. 2013). From both the upper and middle panels, the intensity of pulsations has its daily maximum when the station is at local noon as a result of the direct impact of solar wind pressure on the day-side magnetosphere. Moreover, on March 28, continuous intensive pulsations can be noticed all over the day. This occurs when day side disturbances are followed by magnetotail processes that lead to magnetic field-lines reconnection and plasma acceleration as will be discussed below in this work.

A general overview of the pulsation graph in correlation to the total field, **F** of the lower panel in Figure 6 would explain how pulsations are indicative for magnetic

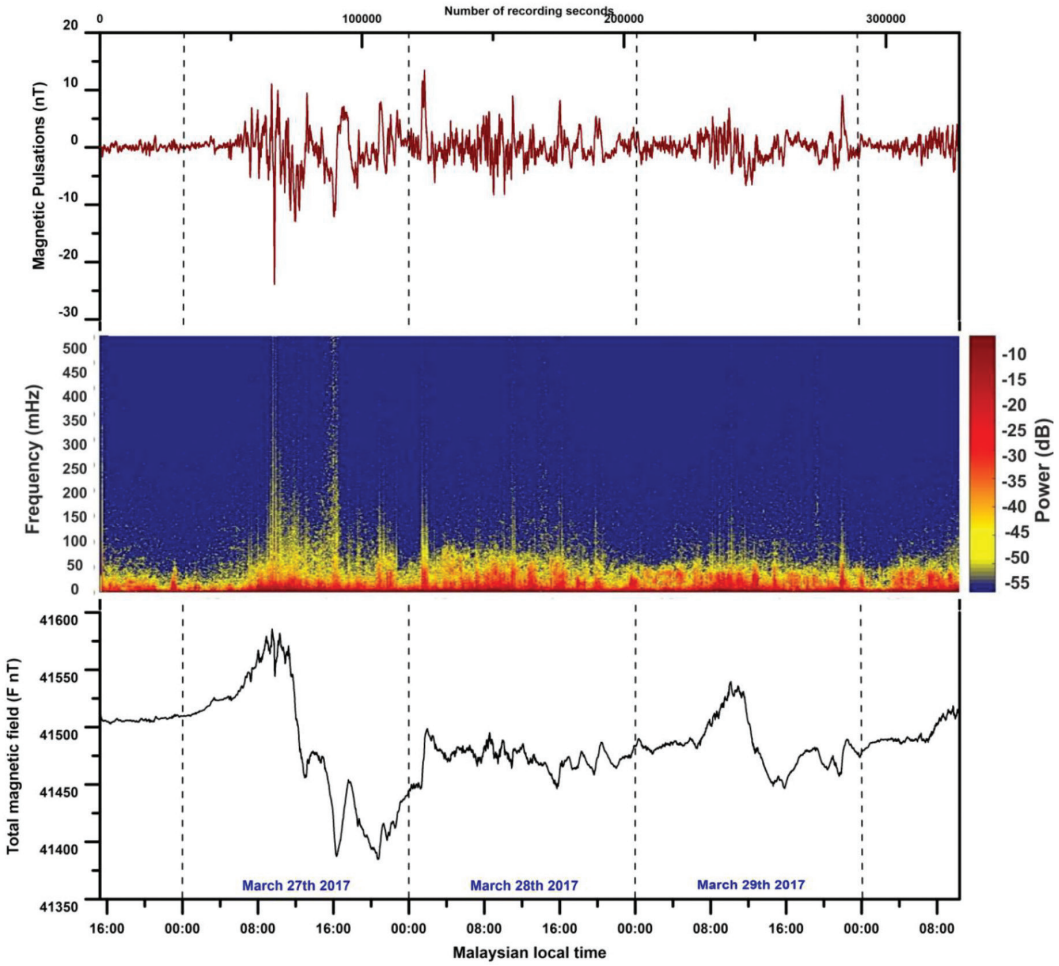

FIGURE 6. (Lower panel) the recorded time series of the total magnetic-field intensity. (Middle panel) the power spectrogram of the magnetic pulsations after a high-pass filtering of the data. (Upper panel) Magnetic pulsations resulted from filtering the long period diurnal variation. The upper and middle panels show a clear increase in pulsations intensity after storm onset. The three panels indicate that despite the recovery of the typical diurnal variation on March 29th the intensive occurrence of pulsations continued

storms. On March 29, the usual diurnal variation form of the total field is almost recovered which might be mistaken as an end of the storm. On the other hand, the sustained occurrence of intensive pulsations gives clue to the ongoing magnetic storm.

MAGNETOSPHERIC BREATHING

When the solar wind density is high, or its speed is accelerated and comes up against the magnetosphere, the magnetosphere gets collision-less compressed. When the wind density is low or its speed is reduced, the magnetosphere expands in space due to the characteristic 'repulsion' property of parallel magnetic field lines. The researchers discovered that the solar wind contains periodic structures of high and low density, driving a periodic 'breathing' action of the magnetosphere and the global generation of magnetic waves (Potemra 1998). Similar breathing activities have been reported for other solar system planets as well (Collier & Lepping 1996; Cowley et al. 2006; Ramer et al. 2016). Breathing is a global phenomenon that affects different parts of the magnetosphere in a differential manner. On the dayside, especially near the subsolar point, it is clearly related to an in-and-out motion of the magnetopause, which is so closely linked to the expansion and contraction of the dayside magnetosphere. The definite response of a ground-based magnetic observatory to a breathing event is a semi-periodic increase and decrease of total field intensity simultaneous with the compression and expansion of the magnetosphere, respectively (Figure 7).

The storm under study exhibits two events of breathing occurrence. One started at 08:00 LT on March 27 and the other started at 08:00 LT on March 28. The first breathing phenomenon is displayed in Figure 8. The total magnetic field started to change semi-periodical with amplitudes from 20nT to a maximum of 40nT with periods of about 40 min.

The fitting polynomial which represents the long-term variation in the magnetosphere is then subtracted from the observed values to get the residual as pure

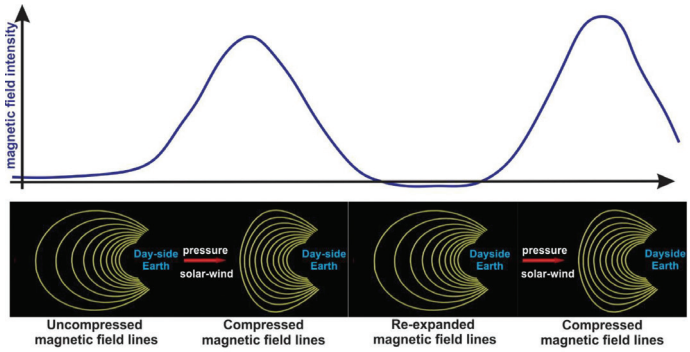

FIGURE 7. Breathing as a global phenomenon that affects different parts of the magnetosphere differently and its response at ground observatories. On the dayside, it is particularly evident in the in-and-out motion of the magnetopause, which is so closely linked to the expansion and contraction of the dayside magnetosphere that the magnetopause position can be used to characterize dayside expansion and contraction. The force of compression is due to enhanced solar wind velocity, whereas the expansion results from the inherent repulsion force between the parallel magnetospheric field-lines. The ground-based observatory response to breathing is a periodic increase and decrease of field intensity with the compression and expansion of the magnetosphere, respectively

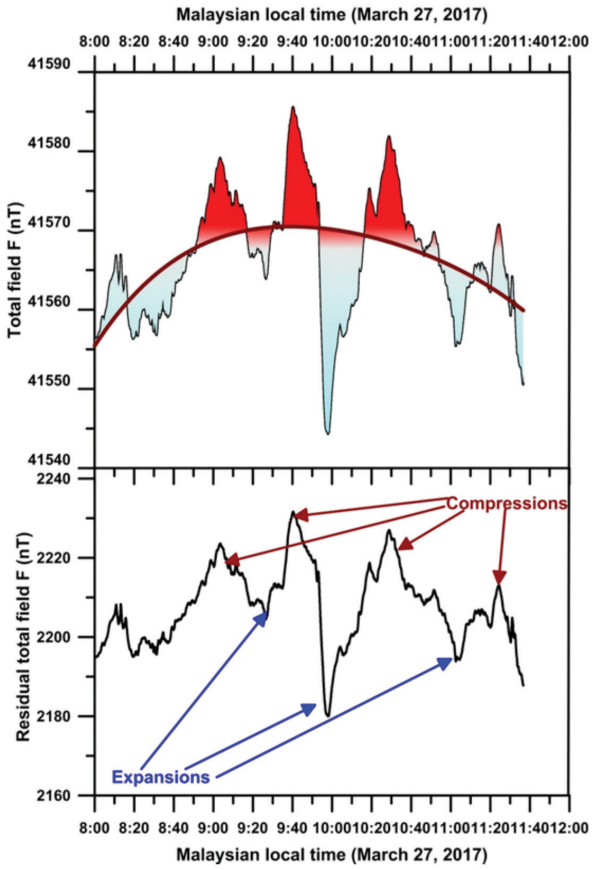

FIGURE 8. The magnetospheric breathing event of March 27. The upper graph shows the recorded total magnetic field intensity from 08:00 to 12:00 LT. The smooth red curve-line is a fitted polynomial of the 4th order that represents longer period variation superimposed on the breathing phenomena. The lower graph is the total field intensity after subtracting the fitted polynomial to display an almost pure breathing phenomenon. The compressions and expansions of the day-side magnetosphere have periods of about 40 min

magnetospheric breathing of compressions and expansions (Figure 8 lower graph). A similar procedure has been applied by Ramer et al. (2016) using a running average on Cassini's observations in Saturn's magnetosphere. Later on March 28 the total field observations showed successive compressions and expansions at 08:00 LT that repeated

itself for 3 times until 09:40 LT (Figure 5). The breathing is particularly superimposed by a gradual semi-linear increase in the total field that could be simply separated by linear fitting.

MAGNETOTAIL RECONNECTION

In addition to the elastic interactions of the solar wind with the magnetosphere such as breathing and pulsations, the reconnection between IMF lines and the geomagnetic field lines at dayside magnetopause and in the magnetotail plays a crucial role in energy injection into the magnetosphere (Wing et al. 2014). Magnetic reconnection is of major impact on substorms and for magnetospheric dynamics (Paschmann et al. 2013).

When the IMF is oriented southward, it tends to reconnect with field lines of the Earth magnetic field at the dayside magnetopause. This process can be considered as a forced reconnection, an interplanetary magnetic field associated with the solar wind plasma flow collides with the Earth's northward field and has no chance to avoid reconnection in the case when two field lines are directed approximately opposite to each other (Figure 9). Therefore, the basic dynamics of the magnetopause reconnection may be mainly controlled by external conditions.

In the magnetotail, a different scenario dominates to lead to reconnection. The antiparallel tail field-lines that relate to their feet at both magnetic poles turn to be overstretched due to the enhanced injection of plasma flows from the dayside solar wind. At a certain limit the stretched field lines collapse and reconnect at an X-line as shown in Figure 9. At the X-line two types of the field- lines originate, an open one that accelerates plasma down-tail and closed field-lines that contract and hence accelerates the plasma earthward. In addition, a westward enhancement of plasma flows is observed by satellites during magnetotail reconnection. These plasma flows were confined to closed field lines and are identified as the ionospheric plasma flow signature of tail reconnection during IMF northward non-substorm intervals (Baumjohann 2002; Nowada et al. 2018; Paschmann et al. 2013; Wing et al. 2014).

On March 28th, as the magnetometer was near midnight (about 01:30 LT) a sudden steep increase in the total field intensity has been observed (Figure 5). As clear from Figure 5, the intensity of the field increased from 41450 nT to 41500 nT within about 10 min. This increase-rate of 5nT/min resembles a form of a shock that leads to compression in magnetic field lines. Such compressional shocks are common on the day side due to common increases in solar wind pressures. However, on the night side, the only possible mechanism of a compressional shock is the contraction of reconnected field lines in the magnetotail. As explained in Figure 9, the X-line at which the field lines reconnect is located far from the Earth's ground due to magnetotail stretching. The stretching forces stop to affect the reconnected lines, which start to shorten itself by moving earthwards and consequently compress the near earth lines.

This scenario would result in a subsequent decrease (recovery) of the total intensity after field-lines relaxation. The time series that is shown in Figure (5) does not represent a clear recovery of the total intensity after reconnection. However, the high-frequency pulsations show the reconnection event as a clear spiky increase associated with a broadband enhancement of pulsations at about 01:40 LT (Figure 6 upper and middle panels). This confirms the occurrence of reconnection simultaneous with an occasional long period increase in the total-field.

SUMMARY AND CONCLUSION

Data from a temporal magnetic station have been utilized to inspect the magnetospheric phenomena occurred as a result of the solar wind interaction. As a first step, the time series are averaged to get 1 Hz sampled data resembles data records available from regular permanent observatories. Once the 1 second data is displayed, it was obvious that the temporal station has recorded the storm in a proper manner in three orthogonal components and provided an accurate calculation of the total magnetic field **F**. The start of the storm is quite determined from the data that continued until the end of the measuring campaign on March 29. The overall view showed that March 28 is the most disturbed day as the typical diurnal variation is totally replaced by irregular perturbations due to magnetotail activity on the night side and a continuous

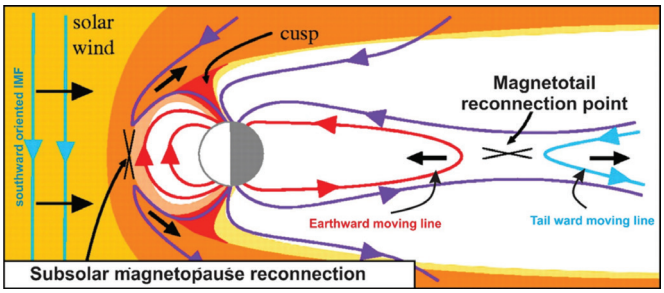

FIGURE 9. Schematic illustration of both day-side (subsolar) reconnection and night-side (magnetotail) reconnection. Magnetotail reconnection occurs when 2 stretched antiparallel field lines merge and result in a tail-ward moving line and an earth-ward moving line. The earthward moving line leads to an abrupt increase in magnetic field intensity on the ground

buffeting of the magnetosphere by energetic solar wind on the dayside.

Detailed consideration showed the occurrence of a magnetotail reconnection event. It is a process that results from the welding of a north-pole field line with a south-pole field line in the overstretched magnetotail due to the additional current densities. The newly originated field-line inherently contracts, compresses near-earth magnetic field-lines and accelerates plasma as well. This event is deduced by a sudden increase of 50nT in the total-field intensity as the station was at 01:30 LT, on the night-side, on March 28. The step form increase is followed by continuous perturbations observed until local dawn.

Magnetic pulsations have a long history as a key feature of storm studies. In order to separate the higher frequency measured pulsations from the long-period variations, a running average of 100 samples is subtracted from the 1 second total field record. The resultant residual pulsations are then studied in the time domain and in the frequency domain by calculating a spectrogram with windows of 1024 samples for the entire observation span. The pulsations give different indications about the classification of the storm. Both, time series and spectrogram display general enhancement of pulsations from the start of the storm to the end of the records. Moreover, characteristic amplification can be noticed near local noon every day which confirms the increased arrival of energetic solar wind from day to day. Especially on March 28 the amplification of pulsations is obvious all over the day. This indicates that in addition to the dayside-triggered perturbations magnetotail processes were also activated due to continuous injections of plasma from the dayside and the generation of additional currents and plasma flows.

The separation of pulsations confirmed the occurrence of the magnetotail reconnection event as an isolated event associated with broadband of amplified pulsations at 01:30 LT on March 28.

Furthermore, two occurrences of magnetospheric breathing have been captured during the storm. Successive increase and decrease in the total intensity at intervals of 10 to several tens of minutes obviously indicate successive compression and expansion of the entire dayside magnetosphere is previously referred to by authors as the breathing of the magnetosphere. The phenomenon on March 27 has been clarified by subtracting a background fitted 4th order polynomial function. The second event on March 28 comprised 3 compressions and expansions starting from 08:00 LT.

Further studies are proposed to utilize satellite data available from different zones in the magnetosphere to understand more about the physics and mechanism of the observed activities. The special location of the station at near-equatorial latitudes would provide a characteristic comparison with satellite data. Regardless of the availability of satellite observations this work exhibits how useful a magnetic observatory can be and how much physics about space weather it can provide at the real time.

REFERENCES

Alfven, H. & Falthammar, C.G. 1963. *Cosmical Electrodynamics: Fundamental Principles*. Oxford: Clarendon Press. p. 228.

Baker, D.N., Pulkkinen, T.I., Angelopulos, V., Baumjohann, W. & McPherron, R.L. 1996. Neutral line model of substorms: Past results and present view. *J. Geophys. Res.* 101(A6): 12875- 13010.

Barnes, A. 1983. Hydromagnetic waves, turbulence, and collisionless processes in the interplanetary medium. In *Solar-Terrestrial Physics: Principles and Theoretical Foundations*, edited by Carovillano, R.L., Forbes, J.M. & Reidel. D. Dordrecht: Publishing Company. pp. 155-199.

Baumjohann, W. 2002. Modes of convection in the magnetotail. *Phys. Plasmas* 9: 3665-3667.

Collier, M.R. & Lepping, R.P. 1996. Jovian magnetopause breathing. *Planetary and Space Science* 44(3): 187-197.

Cowley, S.W.H., Wright, D.M., Bunce, E.J., Carter, A.C., Dougherty, M.K., Giampieri, G., Nichols, J.D. & Robinson, T.R. 2006. Cassini observations of planetary-period magnetic field oscillations in Saturn's magnetosphere: Doppler shifts and phase motion. *Geophys. Res. Lett.* p. 33. DOI: 10.1029/2005GL025522.

Ghamry, E., Lethy, A., Arafa-Hamed, T. & Abd Elaal, E. 2016. A comprehensive analysis of the geomagnetic storms occurred during 18 February and 2 March 2014. *NRIAG Journal of Astronomy and Geophysics* 5(1): 263-268.

Glassmeier, K.H., Soffel, H. & Negendank, J.W. 2009. *Geomagnetic Variations, Space-Time Structure, Processes, and Effects on System Earth*. Heidelberg: Springer Verlag.

Langangen, O., Carlsson, M. & Voort, L.R. 2007. Velocities measured in small-scale solar magnetic elements. *The Astrophysical Journal* 655: 615-623.

Lin, N.M.J.E., Anderson, B.J., McPherron, R.L., Kivelson, M.G., Baumjohann, W., Luehr, H., Potemera, T.A. & Zanetti, L.J. 1991. A comparison of ULF wave fluctuations in the solar wind, magnetosheath, and dayside magnetosphere: 2. Field and plasma conditions in the magnetosheath. *J. Geophys. Res.* 96: 3455-3464.

McPherron, R.L. 2005. Magnetic pulsations: Their sources and relation to solar wind and geomagnetic activity. *Survey of Geophysics* 26: 545-592.

Nabert, C., Glassmeier, K.H. & Plaschke, F. 2013. A new method for solving the MHD equations in the magnetosheath. *Ann. Geophys.* 31: 419-437.

Nabert, C., Othmer, C. & Glassmeier, K.H. 2017. Estimating a planetary magnetic field with time-dependent global MHD simulations using an adjoint approach. *Geophys.* 35: 613-628.

Nowada, M., Fear, R.C., Grocott, A., Shi, Q.Q., Yang, J. & Zong, Q.G. 2018. Subsidence of ionospheric flows triggered by magnetotail magnetic reconnection during transpolar arc brightening. *Journal of Geophysical Research: Space Physics* 123: 3398-3420.

Paschmann, G., Oieroset, M. & Phan, T. 2013. *In situ* observations of reconnection in space. *Sci. Rev.* 178: 385-417.

Potemra, T.A. 1998. The dynamic magnetosphere. In *Polar Cap Boundary Phenomena. NATO ASI Series (Series C: Mathematical and Physical Sciences)*, edited by Moen, J., Egeland, A. & Lockwood, M. Dordrecht: Springer. p. 509.

Ramer, K.M., Kivelson, M.G., Sergis, N., Khurana, K.K. & Jia, X. 2016. Spinning, breathing, and flapping: Periodicities in Saturn's middle magnetosphere. *J. Geophys. Res.* pp. 122-126.

Schillinger, D. & Papadopoulos, V. 2010. Accurate estimation of evolutionary power spectra for strongly narrow-band random fields. *Computer Methods in Applied Mechanics and Engineering* 199: 947-960.

Schillinger, D., Stefanov, D. & Stavrev, A. 2013. The method of separation for evolutionary spectral density estimation of multi-variate and multi-dimensional non-stationary stochastic processes. *Probabilistic Engineering Mechanics* 33: 58-78.

Wing, S., Johnson, J.R., Chaston, C.C., Echim, M., Escoubet, C.P., Lavraud, B., Lemon, C., Nykyri, K., Otto, A., Raeder, J. & Wang, C.P. 2014. Review of solar wind entry into and transport within the plasma sheet. *Space Sci. Rev.* 184: 33-86.

Arafa-Hamed, T.
National Research Institute of Astronomy and Geophysics (NRIAG)
Egypt

Khalil, A.* & Nawawi, M.
School of Physics
Universiti Sains Malaysia
11800 USM, Pulau Pinang
Malaysia

Hassan, H.
Geology Department
Faculty of Science
Helwan University
Egypt

M.H. Arifin
Program Geologi, Pusat Sains Bumi dan Alam Sekitar
Fakulti Sains dan Teknologi
Universiti Kebangsaan Malaysia
43600 UKM Bangi, Selangor Darul Ehsan
Malaysia

*Corresponding author; email: amin_khalil@usm.my

Received: 7 April 2019
Accepted: 15 August 2019